

Novel R tools for analysis of genome-wide population genetic data with emphasis on clonality

Zhian N. Kamvar¹, Jonah C. Brooks², Niklaus J. Grünwald^{1,3*}

¹ Botany and Plant Pathology, Oregon State University, Corvallis, OR, USA

² College of Electrical Engineering and Computer Science, Oregon State University, Corvallis, OR, USA

³ Horticultural Crops Research Laboratory, USDA-Agricultural Research Service, Corvallis, OR, USA

Correspondence*:

Niklaus J. Grünwald
Horticultural Crops Research Laboratory USDA ARS
3420 NW Orchard Ave.
Corvallis, OR, 97330, grunwalg@science.oregonstate.edu

2 ABSTRACT

To gain a detailed understanding of how plant microbes evolve and adapt to hosts, pesticides, and other factors, knowledge of the population dynamics and evolutionary history of populations is crucial. Plant pathogen populations are often clonal or partially clonal which requires different analytical tools. With the advent of high throughput sequencing technologies, obtaining genome-wide population genetic data has become easier than ever before. We previously contributed the R package *poppr* specifically addressing issues with analysis of clonal populations. In this paper we provide several significant extensions to *poppr* with a focus on large, genome-wide SNP data. Specifically, we provide several new functionalities including the new function `mlg.filter` to define clone boundaries allowing for inspection and definition of what is a clonal lineage, a sliding-window analysis of the index of association, modular bootstrapping of any genetic distance, and analyses across any level of hierarchies.

Keywords: clonality, population genomics, bootstrap, index of association, hierarchical analysis, sliding window

INTRODUCTION

To paraphrase Dobzhansky, nothing in the field of plant-microbe interactions makes sense except in the light of population genetics (Dobzhansky, 1973). Genetic forces such as selection and drift act on alleles in a population. Thus, a true understanding of how plant pathogens emerge, evolve and adapt to crops, fungicides, or other factors, can only be elucidated in the context of population level phenomena given the demographic history of populations (McDonald and Linde, 2002; Grünwald and Goss, 2011; Milgroom et al., 1989). The field of population genetics, in the era of whole genome resequencing, provides unprecedented power to describe the evolutionary history and population processes that drive coevolution between pathogens and hosts. This powerful field thus critically enables effective deployment of R genes, design of pathogen informed plant resistance breeding programs, and implementation of fungicide rotations that minimize emergence of resistance.

Most computational tools for population genetics are based on concepts developed for sexual model organisms. Populations that reproduce clonally or are polyploid are thus difficult to characterize using

27 classical population genetic tools because theoretical assumptions underlying the theory are violated. Yet,
28 many plant pathogen populations are at least partially clonal if not completely clonal (Milgroom, 1996;
29 Anderson and Kohn, 1995). Thus, development of tools for analysis of clonal or polyploid populations is
30 needed.

31 Genotyping by sequencing and whole genome resequencing provide the unprecedented ability to
32 identify thousands of single nucleotide polymorphisms (SNPs) in populations (Elshire et al., 2011; Luikart
33 et al., 2003; Davey et al., 2011). With traditional marker data (e.g., SSR, AFLP) a clone was typically
34 defined as a unique multilocus genotype (MLG) (Grünwald and Hoheisel, 2006; Falush et al., 2003; Goss
35 et al., 2009; Cooke et al., 2012; Taylor and Fisher, 2003). Availability of large SNP data sets provides new
36 challenges for data analysis. These data are based on reduced representation libraries and high throughput
37 sequencing with moderate sequencing depth which invariably results in substantial missing data, error in
38 SNP calling due to sequencing error, lack of read depth or other sources of spurious allele calls (Mastretta-
39 Yanes et al., 2015). It is thus not clear what a clone is in large SNP data sets and novel tools are required
40 for definition of clone boundaries.

41 The research community using the R statistical and computing language (R Core Team, 2015) has
42 developed a plethora of new resources for population genetic analysis (Paradis, 2010; Jombart, 2008).
43 R is particularly appealing because all code is open source and functions can be evaluated and modified
44 by any user. Recently, we introduced the R package *poppr* specifically developed for analysis of clonal
45 populations (Kamvar et al., 2014b). *Poppr* previously introduced several novel features including the
46 ability to conduct a hierarchical analysis across unlimited hierarchies, test for linkage association, graph
47 minimum spanning networks or provide bootstrap support for Bruvo's distance in resulting trees. *Poppr*
48 has been rapidly adopted and applied to a range of studies including for example horizontal transmission
49 in leukemia of clams (Metzger et al., 2015), study of the vector-mediated parent-to-offspring transmission
50 in an avian malaria-like parasite (Chakarov et al., 2015), and characterization of the emergence of the
51 invasive forest pathogen *Hymenoscyphus pseudoalbidus* (Gross et al., 2014). It has also been used to
52 implement real-time, online shinyR based tools for visualizing relationships among unknown MLGs in
53 reference databases (<http://phytophthora-id.org/>) (Grünwald et al., 2011).

54 Here, we introduce *poppr* 2.0, which provides a major update to *poppr* (Kamvar et al., 2014b) including
55 novel tools for analysis of clonal populations specifically addressing large SNP data. Significant novel
56 tools include functions for calculating clone boundaries and collapsing individuals into clonal groups
57 based on a user-specified genetic distance threshold, sliding window analyses, genotype accumulation
58 curves, reticulations in minimum spanning networks, and bootstrapping for any genetic distance.

IMPLEMENTATIONS AND EXAMPLES

CLONAL IDENTIFICATION

59 As highlighted in previous work, clone correction is an important component of population genetic
60 analysis of organisms that are known to reproduce asexually (Kamvar et al., 2014b; Milgroom, 1996;
61 Grünwald et al., 2003). This method is a partial correction for bias that affects metrics that rely on allele
62 frequencies assuming panmixia. It was initially designed for data with only a handful of markers. With the
63 advent of large-scale sequencing and reduced- representation libraries, it has become easier to sequence
64 tens of thousands of markers from hundreds of individuals (Elshire et al., 2011; Davey et al., 2011; Davey
65 and Blaxter, 2010). With this larger number of markers, the genetic resolution is much greater, but the
66 chance of genotyping error is also greatly increased and missing data is frequent (Mastretta-Yanes et al.,
67 2015). Taking this fact and occasional somatic mutations into account, it would be impossible to separate
68 true clones from independent individuals by just comparing what MLGs are different. We introduce a
69 new method for collapsing unique multilocus genotypes determined by naive string comparison into
70 multilocus lineages utilizing any genetic distance given three different clustering algorithms: farthest
71 neighbor, nearest neighbor, and UPGMA (average neighbor) (Sokal, 1958).

These clustering algorithms act on a distance matrix that is either provided by the user or generated via a function that will calculate a distance from genclone objects such as `bruvo.dist`, which in particular applies to any level of ploidy (Bruvo et al., 2004). All algorithms have been implemented in C and utilize the OpenMP framework for optional parallel processing (Dagum and Menon, 1998). Default is the conservative farthest neighbor algorithm (Fig. 1A), which will only cluster samples together if all samples in the cluster are at a distance less than the given threshold. By contrast, the nearest neighbor algorithm will have a chaining effect that will cluster samples akin to adding links on a chain where a sample can be included in a cluster if all of the samples have at least one connection below a given threshold (Fig. 1C). The UPGMA, or average neighbor clustering algorithm is the one most familiar to biologists as it is often used to generate ultra-metric trees based on genetic distance (Fig. 1B). This algorithm will cluster by creating a representative sample per cluster and joining clusters if these representative samples are closer than the given threshold.

We utilize data from the microbe *Phytophthora infestans* to show how the `mlg.filter` function collapses multilocus genotypes with Bruvo's distance assuming a genome addition model (Bruvo et al., 2004). *P. infestans* is the causal agent of potato late blight originating from Mexico that spread to Europe in the mid 19th century (Goss et al., 2014; Yoshida et al., 2013). *P. infestans* reproduces both clonally and sexually. The clonal lineages of *P. infestans* have been formally defined into 18 separate clonal lineages using a combination of various molecular methods including AFLP and microsatellite markers (Lees et al., 2006; Li et al., 2013). For these data, we used `mlg.filter` to detect all of the distance thresholds at which 18 multilocus lineages would be resolved. We used these thresholds to define multilocus lineages and create contingency tables and dendograms to determine how well the multilocus lineages were detected.

For the *P. infestans* population, the three algorithms were able to detect 18 multilocus lineages at different distance thresholds (Fig. 2). Contingency tables between the described multilocus genotypes and the genotypes defined by distance show that most of the 18 lineages were resolved, except for US-8, which is polytomic (Table 1).

We utilized simulated data to evaluate the effect of sequencing error and missing data on MLG calling. We constructed the data using the `glSim` function in *aedgenet* (Jombart and Ahmed, 2011) to obtain a SNP data set for demonstration. Two diploid data sets were created, each with 10k SNPs (25% structured into two groups) and 200 samples with 10 ancestral populations of even sizes. Clones were created in one data set by marking each sample with a unique identifier and then randomly sampling with replacement. It is well documented that reduced- representation sequencing can introduce several erroneous calls and missing data (Mastretta-Yanes et al., 2015). To reflect this, we mutated SNPs at a rate of 10% and inserted an average of 10% missing data for each sample after clones were created, ensuring that no two sequences were alike. The number of mutations and missing data per sample were determined by sampling from a Poisson distribution with $\lambda = 1000$. After pooling, 20% of the data set was randomly sampled for analysis. Genetic distance was obtained with the function `bitwise.dist`, which calculates the fraction of different sites between samples equivalent to Provesti's distance, counting missing data as equivalent in comparison (Prevosti et al., 1975).

All three filtering algorithms were run with a threshold of 1, returning a numeric vector of length $n - 1$ where each element represented a threshold at which two samples/clusters would join. Since each data set would have varying distances between samples, the clonal boundary threshold was defined as the midpoint of the largest gap between two thresholds that collapsed less than 50% of the data.

Out of the 100 simulations run, we found that across all methods, detection of duplicated samples had ~ 98% true positive fraction and ~ 0.8% false positive fraction indicating that this method is robust to simulated populations.

MINIMUM SPANNING NETWORKS WITH RETICULATION

118 In its original iteration, *poppr* introduced minimum spanning networks that were based on the *igraph*
119 function `minimum.spanning.tree` (Csardi and Nepusz, 2006). This algorithm produces a minimum
120 spanning tree with no reticulations where nodes represent individual MLGs. In other minimum spanning
121 network programs, reticulation is obtained by calculating the minimum spanning tree several times and
122 returning the set of all edges included in the trees. Due to the way *igraph* has implemented Prim's
123 algorithm, it is not possible to utilize this strategy, thus we implemented an internal C function to walk
124 the space of minimum spanning trees based on genetic distance to connect groups of nodes with edges of
125 equal weight.

126 To demonstrate the utility of minimum spanning networks with reticulation, we used two clonal data
127 sets: the H3N2 flu virus data from the *adegenet* package using years of each epidemic as the population
128 factor, and *Phytophthora ramorum* data from Nurseries and Oregon forests (Jombart et al., 2010; Kamvar
129 et al., 2014a). Minimum spanning networks were created with and without reticulation using the *poppr*
130 functions `diss.dist` and `bruvo.msn` for the H3N2 and *P. ramorum* data, respectively (Kamvar et
131 al., 2014b; Bruvo et al., 2004). To detect mlg clusters, the infoMAP community detection algorithm was
132 applied with 10,000 trials as implemented in the R package *igraph* version 0.7.1 utilizing genetic distance
133 as edge weights and number of samples in each MLG as vertex weights (Csardi and Nepusz, 2006; Rosvall
134 and Bergstrom, 2008).

135 To evaluate the results, we compared the number, size, and entropy (H) of the resulting communities
136 as we expect a highly clonal organism with low genetic diversity to result in a few, large communities.
137 We also created contingency tables of the community assignments with the defined populations and used
138 those to calculate entropy using Shannon's index with the function `diversity` from the R package
139 *vegan* version 2.2-1 (Oksanen et al., 2015; Shannon, 2001). A low entropy indicates presence of a few
140 large communities whereas high entropy indicates presence of many small communities.

141 The infoMAP algorithm revealed 63 communities with a maximum community size of 77 and $H = 3.56$
142 for the reticulate network of the H3N2 data and 117 communities with a maximum community size of
143 26 and $H = 4.65$ for the minimum spanning tree. The entropy across years was greatly decreased for
144 all populations with the reticulate network compared to the minimum spanning tree (Fig. 3). Note that
145 the reticulated network (Fig. 3B) showed patterns corresponding with those resulting from a discriminant
146 analysis of principal components (Fig. 3D) (Jombart et al., 2010).

147 Graph walking of the reticulated minimum spanning network of *P. ramorum* by the infoMAP algorithm
148 revealed 16 communities with a maximum community size of 13 and $H = 2.60$. The un-reticulated
149 minimum spanning tree revealed 20 communities with a maximum community size of 7 and $H = 2.96$.
150 In the ability to predict Hunter Creek as belonging to a single community, the reticulated network was
151 successful whereas the minimum spanning tree separated one genotype from that community. The entropy
152 for the reticulated network was lower for all populations except for the coast population (supplementary
153 information).

BOOTSTRAPPING

154 Assessing population differentiation through methods such as G_{st} , AMOVA, and Mantel tests relies on
155 comparing samples within and across populations (Nei, 1973; Excoffier et al., 1992; Mantel, 1967).
156 Confidence in distance metrics is related to the confidence in the markers to accurately represent the
157 diversity of the data. Especially true with microsatellite markers, a single hyper-diverse locus can make a
158 population appear to have more diversity based on genetic distance. Using a bootstrapping procedure of
159 randomly sampling loci with replacement when calculating a distance matrix provides support for clades
160 in hierarchical clustering.

161 Data in `genind` and `genpop` objects are represented as matrices with individuals in rows and alleles in
162 columns (Jombart, 2008). This gives the advantage of being able to use R's matrix algebra capabilities

163 to efficiently calculate genetic distance. Unfortunately, this also means that bootstrapping is a non-trivial
 164 task as all alleles at a single locus need to be sampled together. To remedy this, we have created an internal
 165 S4 class called “bootgen”, which extends the internal “gen” class from *adegenet*. This class can be created
 166 from any genind, genclone, or genpop object, and allows loci to be sampled with replacement. To further
 167 facilitate bootstrapping, a function called *aboot*, which stands for “any boot”, is introduced that will
 168 bootstrap any genclone, genind, or genpop object with any genetic distance that can be calculated from it.

169 To demonstrate calculating a dendrogram with bootstrap support, we used the *poppr* function *aboot*
 170 on population allelic frequencies derived from the data set *microbov* in the *adegenet* package with
 171 1000 bootstrap replicates (Jombart, 2008; Laloë et al., 2007). The resulting dendrogram shows bootstrap
 172 support values > 50% (Fig. 4) and used the following code:

```
library("poppr")
data("microbov", package = "adegenet")
strata(microbov) <- data.frame(other(microbov))
setPop(microbov) <- ~coun/spe/breed
bov_pop <- genind2genpop(microbov)

set.seed(20150428)
pop_tree <- aboot(bov_pop, sample = 1000, cutoff = 50)
```

GENOTYPE ACCUMULATION CURVE

173 Analysis of population genetics of clonal organisms often borrows from ecological methods such as
 174 analysis of diversity within populations (Milgroom, 1996; Arnaud-Hanod et al., 2007; Grünwald et al.,
 175 2003). When choosing markers for analysis, it is important to make sure that the observed diversity in your
 176 sample will not appreciably increase if an additional marker is added (Arnaud-Hanod et al., 2007). This
 177 concept is analogous to a species accumulation curve, obtained by rarefaction. The genotype accumulation
 178 curve in *poppr* is implemented in the function *genotype_curve*. The curve is constructed by randomly
 179 sampling x loci and counting the number of observed MLGs. This repeated r times for 1 locus up to $n - 1$
 180 loci, creating $n - 1$ distributions of observed MLGs.

181 The following code example demonstrates the genotype accumulation curve for data from Everhart and
 182 Scherm (2015) showing that these data reach a small plateau and have a greatly decreased variance with
 183 12 markers, indicating that there are enough markers such that adding more markers to the analysis will
 184 not create very many new genotypes (Fig. 5).

```
library("poppr")
library("ggplot2")
data("monpop", package = "poppr")

set.seed(20150428)
genotype_curve(monpop, sample = 1000)
p <- last_plot() + theme_bw() # get the last plot
p + geom_smooth(aes(group = 1)) # plot with a trendline
```

INDEX OF ASSOCIATION

185 The index of association (I_A) is a measure of multilocus linkage disequilibrium that is most often used
 186 to detect clonal reproduction within organisms that have the ability to reproduce via sexual or asexual
 187 processes (Brown et al., 1980; Smith et al., 1993; Milgroom, 1996). It was standardized in 2001 as
 188 \bar{r}_d by Agapow and Burt (2001) to address the issue of scaling with increasing number of loci. This
 189 metric is typically applied to traditional dominant and co-dominant markers such as AFLPs, SNPs, or

190 microsatellite markers. With the advent of high throughput sequencing, SNP data is now available in a
191 genome-wide context and in very large matrices including thousands of SNPs. For this reason, we devised
192 two approaches using the index of association for large numbers of markers typical for population genomic
193 studies. Both functions utilize *adegenet*'s "genlight" object class, which efficiently stores 8 binary alleles
194 in a single byte (Jombart and Ahmed, 2011). As calculation of the \bar{r}_d requires distance matrices of absolute
195 number of differences, we utilize a function that calculates these distances directly from the compressed
196 data called `bitwise.dist`.

197 The first approach is a sliding window analysis implemented in the function `win.ia`. It utilizes the
198 position of markers in the genome to calculate \bar{r}_d among any number of SNPs found within a user-
199 specified windowed region. It is important that this calculation utilize \bar{r}_d as the number of loci will be
200 different within each window (Agapow and Burt, 2001). This approach would be suited for a quick
201 calculation of linkage disequilibrium across the genome that can detect potential hotspots of LD that
202 could be investigated further with more computationally intensive methods assuming that the number of
203 samples << the number of loci.

204 As it would necessarily focus on loci within a short section of the genome that may or may not
205 be recombining, a sliding window approach would not be good for utilizing \bar{r}_d as a test for clonal
206 reproduction. A remedy for this is implemented in the function `samp.ia`, which will randomly sample
207 m loci, calculate \bar{r}_d , and repeat r times, thus creating a distribution of expected values of \bar{r}_d .

208 To demonstrate the sliding window and random sampling of \bar{r}_d with respect to clonal populations, we
209 simulated two populations containing 1,100 neutral SNPs for 100 diploid individuals under the same
210 initial seed. One population had individuals randomly sampled with replacement, representing the clonal
211 population. After sampling, both populations had 5% random error and 1% missing data independently
212 propagated across all samples. On average, we obtained a higher value of \bar{r}_d for the clonal population
213 compared to the sexual population for both methods (Fig. 6).

DATA FORMAT UPDATES: POPULATION STRATA AND HIERARCHIES

214 Assessments of population structure through methods such as hierarchical F_{st} (Goudet, 2005) and
215 AMOVA (Michalakis and Excoffier, 1996) require hierarchical sampling of populations across space
216 or time (Linde et al., 2002; Everhart and Scherm, 2015; Grünwald and Hoheisel, 2006). With clonal
217 organisms, basic practice has been to clone-censor data to avoid downward bias in diversity due to
218 duplicated genotypes that may or may not represent different samples (Milgroom, 1996). This correction
219 should be performed with respect to a population hierarchy to accurately reflect the biology of the
220 organism. Traditional data structures for population genetic data in most analysis tools allow for only
221 one level of hierarchical definition. The investigator thus had to provide the data set for analysis at each
222 hierarchical level.

223 To facilitate handling hierarchical and multilocus genotypic metadata, *poppr* version 1.1 introduced
224 a new S4 data object called "genclone", extending *adegenet*'s "genind" object (Kamvar and Grünwald,
225 unpublished). The genclone object formalized the definitions of multilocus genotypes and population
226 hierarchies by adding two slots called "mlg" and "hierarchy" that carried a numeric vector and a data
227 frame, respectively. These new slots allow for increased efficiency and ease of use by allowing these
228 metadata to travel with the genetic data. The hierarchy slot in particular contains a data frame where each
229 column represents a separate hierarchical level. This is then used to set the population factor of the data by
230 supplying a hierarchical formula containing one or more column names of the data frame in the hierarchy
231 slot.

232 The functionality represented by the hierarchy slot has now been migrated from the *poppr* to the
233 *adegenet* package version 2.0 to allow hierarchical analysis in *adegenet*, *poppr*, and other dependent
234 packages. The prior *poppr* hierarchy slot and methods have now been renamed `strata` in *adegenet*.
235 A short example of the utility of these methods can be seen in the code segment under **Bootstrapping**,

236 above. This migration provides end users with a broader ability to analyze data hierarchically in R across
237 packages.

AVAILABILITY

238 As of this writing, the *poppr* R package version 2.0 containing all of the features described here
239 is located at <https://github.com/grunwaldlab/poppr/tree/2.0-rc>. It is necessary
240 to install *adegenet* 2.0 before installing *poppr*. It can be found at <https://github.com/thibautjombart/adegenet>. Both of these can be installed via the R package *devtools* (Wickham
241 and Chang, 2015).

REQUIREMENTS

243 • R version 3.0 or better
244 • A C compiler. For windows, this can be obtained via Rtools (<http://cran.r-project.org/bin/windows/Rtools/>). On OSX, this can be obtained via Xcode. For parallel support, gcc
245 version 4.6 or better is needed.
246

INSTALLATION

247 From within R, *poppr* can be installed via:

```
install.packages("devtools")
library("devtools")
install_github("thibautjombart/adegenet")
install_github("grunwaldlab/poppr@2.0-rc")
```

248 Several population genetics packages in R are currently going through a major upgrade
249 following the 2015 R hackathon on population genetics (<https://github.com/NESCent/r-popgen-hackathon>) and have not yet been updated in CRAN. We will upload *poppr* 2.0 to CRAN
250 once all other reverse dependent packages have been updated.
251

DISCUSSION

252 Given low cost and high throughput of current sequencing technologies we are entering a new era of
253 population genetics where large SNP data sets with thousands of markers are becoming available for large
254 populations in a genome-wide context. This data provides new possibilities and challenges for population
255 genetic analyses. We provide novel tools that enable analysis of this data in R with a particular emphasis
256 on clonal organisms.

257 Particularly useful is the implementation of \bar{r}_d in a genomic context (Agapow and Burt, 2001). Random
258 sampling of loci across the genome can give an expected distribution of \bar{r}_d , which is expected to have
259 a mean of zero for panmictic populations. This metric is not affected by the number of loci sampled, is
260 model free, and has the ability to detect population structure. Thus, \bar{r}_d is also implemented for sliding
261 window analyses that are useful to detect candidate regions of linkage disequilibrium for further analysis.

262 Clustering multilocus genotypes into multilocus lineages based on genetic distances is a non-trivial task
263 given large SNP data sets. Moreover, this has not previously been implemented for genomic data for
264 clonal populations. Clonal assignment has previously been available in the programs GENCLONE and
265 GENODIVE for classical markers (Arnaud-Hanod et al., 2007; Meirmans and Van Tienderen, 2004). Our
266 method with `mlg.filter` builds upon this idea and allows the user to choose between three different

267 approaches for clustering MLGs. As diagrammed in Fig. 1 and demonstrated in Fig. 2, it is clear that the
268 choice of clustering algorithm has an impact on the data, where for example a genetic distance cutoff of
269 0.1 would be the difference between 14 multilocus lineages (MLLs) and 17 MLLs for nearest neighbor
270 and UPGMA clustering, respectively (Fig. 2). The option to choose the clustering algorithm gives the
271 user the ability to choose what is biologically relevant to their populations. While there is not one optimal
272 procedure for defining boundaries in clonal lineages, our tool provides a means of exploring the potential
273 MLG or MLL boundary space.

274 Minimum spanning networks are a useful tool to analyze the relationships between individuals in a
275 population because each node represents an observed sample and they can have multiple edges (as
276 opposed to bifurcating dendrograms where only tips represent samples). Minimum spanning networks
277 by default are constructed without loops, but for clonal organisms, this often results in a minimum
278 spanning network that becomes a chain, implying that the clones were derived in a progressive and linear
279 fashion. This presents but one potential scenario for clonal organisms, but does not account for any other
280 biologically relevant process. Reticulations in the minimum spanning networks allow for a representation
281 of uncertainty that goes along with clonal organisms. The current implementation in *poppr* has been
282 successfully used in analyses such as reconstruction of the *P. ramorum* epidemic in Curry County, OR
283 (Kamvar et al., 2014a, 2015). Reticulated networks also allow for the application of graph community
284 detection algorithms such as the infoMAP algorithm (Rosvall and Bergstrom, 2008). As shown in the *P.*
285 *ramorum* and H3N2 data, while it is possible to utilize these graph walking algorithms on non-reticulate
286 minimum spanning trees, the results derived from these are limited to explain populations derived from
287 serial cloning events.

288 *Poppr* 2.0 is open source and available on GitHub. Members of the community are invited to contribute
289 by raising issues or pull requests on our repository at [https://github.com/grunwaldlab/
290 poppr/issues](https://github.com/grunwaldlab/poppr/issues).

ACKNOWLEDGEMENTS

291 We thank Ignazio Carbone for discussions on the index of association; David Cooke, Sanmohan Baby,
292 and Jens Hansen for beta testing; and Thibaut Jombart for allowing us to incorporate the strata
293 slot and related methods in *adegenet*. We also thank all the members of the 2015 R hackathon on
294 population genetics in Durham, NC for their advice and input ([https://github.com/NESCent/
295 r-popgen-hackathon](https://github.com/NESCent/r-popgen-hackathon)). This work was supported in part by US Department of Agriculture (USDA)
296 Agricultural Research Service Grant 5358-22000-039-00D, USDA APHIS, the USDA-ARS Floriculture
297 Nursery Initiative, and the USDA-Forest Service Forest Health Monitoring Program.

CONFLICT OF INTEREST STATEMENT

298 The authors declare no observable conflict of interest.

AUTHOR CONTRIBUTIONS

299 ZK and JB wrote, tested, and maintained the code. ZK and NG wrote the manuscript.

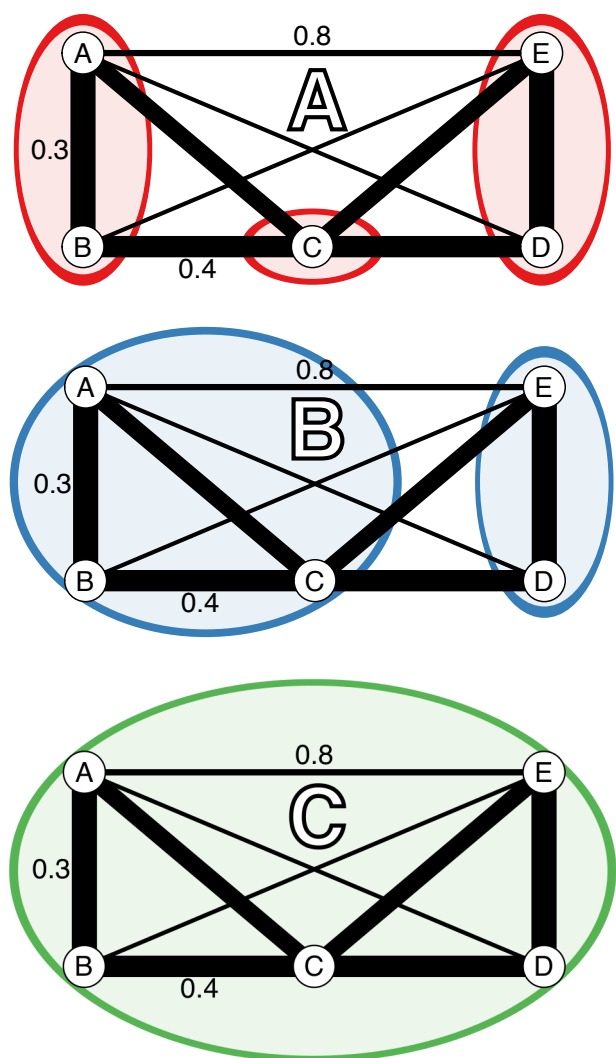
FIGURES AND TABLES**FIGURE 1**

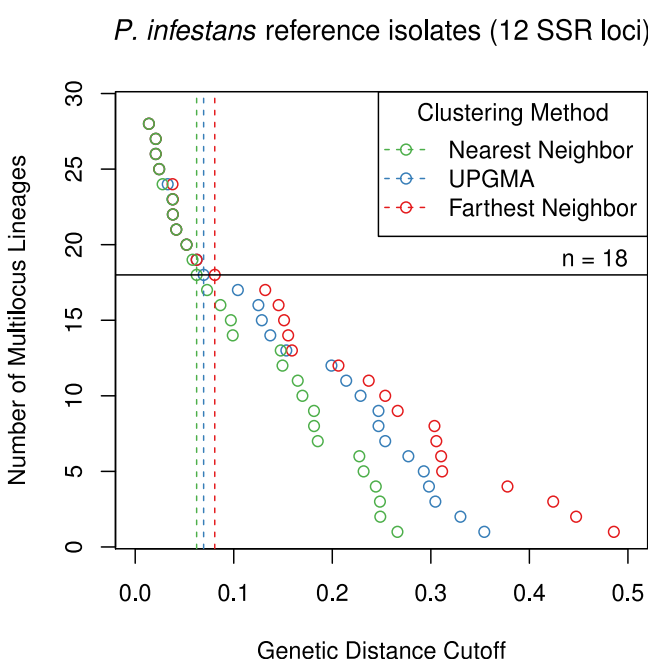
FIGURE 2

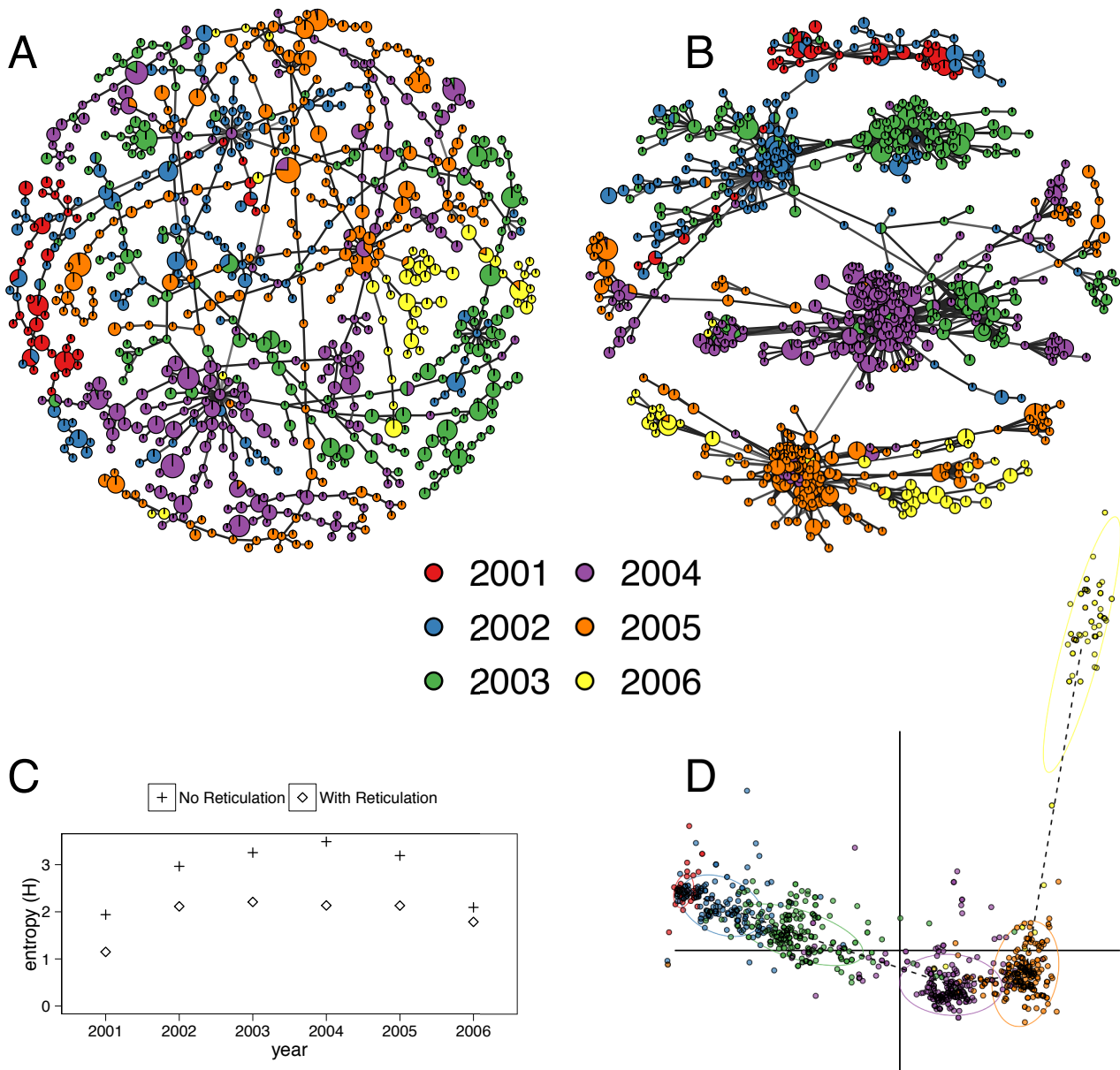
FIGURE 3

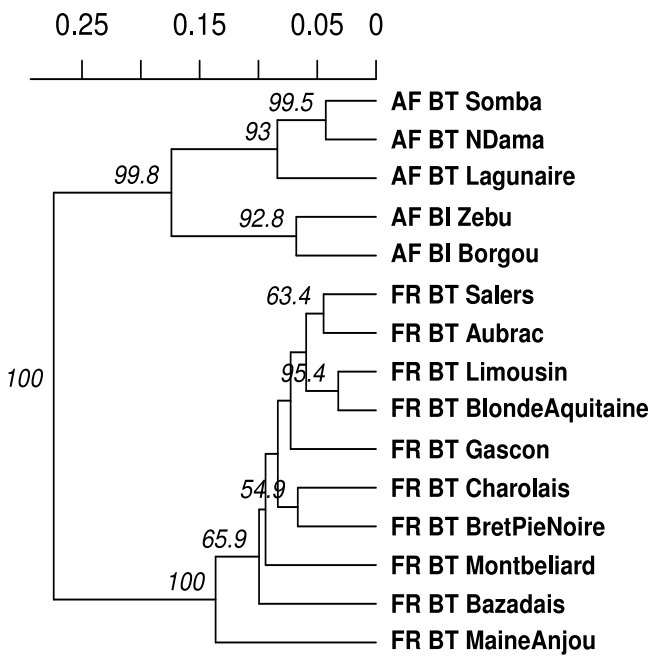
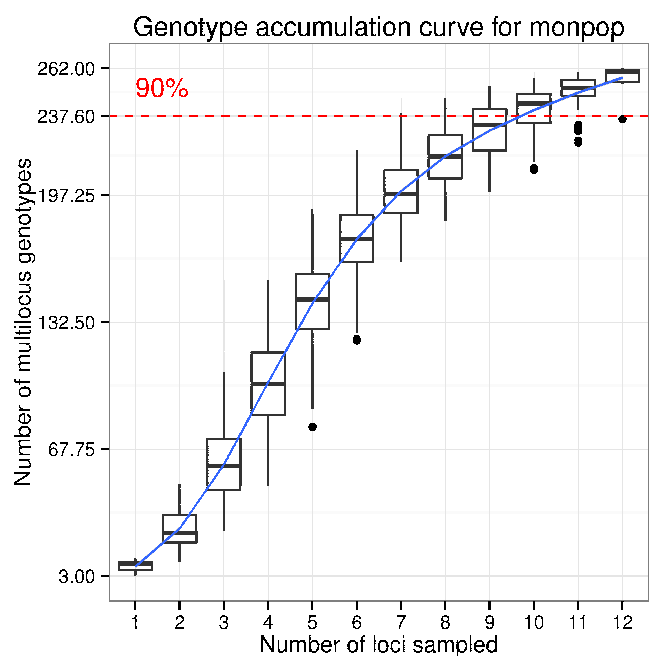
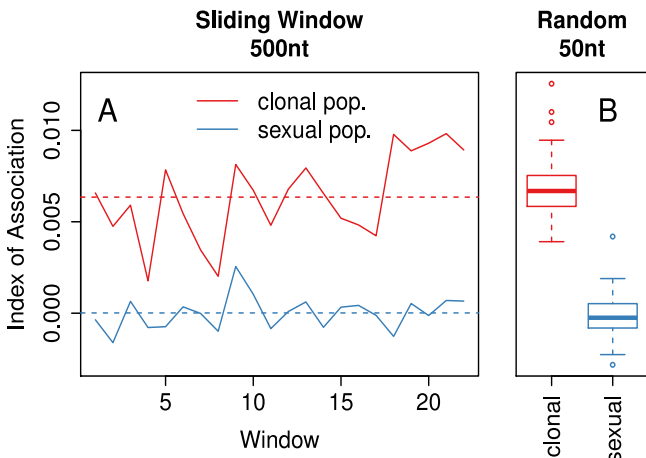
FIGURE 4**FIGURE 5**

FIGURE 6

305

306 **Table 1** Contingency table comparing multilocus lineages assigned based on average neighbor clustering
307 (columns) vs. multilocus lineages defined in Li et al. (2013) and Lees et al. (2006).

	3	4	5	6	8	10	12	15	16	17	18	20	21	22	24	25	27	28
B	1	.	.
C	1	.	.	.
D.1	1	.	.	.
D.2	1	.	.	.
EU-13	1
EU-4	1
EU-5	2
EU-8	1
US-11	2	.	.
US-12	.	1
US-14	1
US-17	1
US-20	2
US-21	2	.	.
US-22	2
US-23	3
US-24	.	.	.	3
US-8	.	.	1	1	.	2

FIGURE LEGENDS

308 **Figure 1** Diagrammatic representation of the three clustering algorithms implemented in `m1g.filter`.
309 (A-C) Represent different clustering algorithms on the same imaginary network with a threshold of 0.451.
310 Edge weights are represented in arbitrary units noted by the line thickness and numerical values next to
311 the lines. All outer angles are 90 degrees, so the un-labeled edge weights can be obtained with simply
312 geometry. Colored circles represent clusters of genotypes. (A) Farthest neighbor clustering does not cluster
313 nodes B and C because nodes A and C are more than a distance of 0.451 apart. (B) UPGMA (average
314 neighbor) clustering clusters nodes A, B, and C together because the average distance between them and

315 C is < 0.451 . (C) Nearest neighbor clustering clusters all nodes together because the minimum distance
 316 between them is always < 0.451 .

317 **Figure 2** Graphical representation of three different clustering algorithms collapsing multilocus
 318 genotypes for 12 SSR loci from *Phytophthora infestans* representing 18 clonal lineages. The horizontal
 319 axis is Bruvo's genetic distance assuming the genome addition model. The vertical axis represents the
 320 number of multilocus lineages observed. Each point shows the threshold at which one would observe a
 321 given number of multilocus genotypes. The horizontal black line represents 18 multilocus genotypes and
 322 vertical dashed lines mark the thresholds used to collapse the multilocus genotypes into 18 multilocus
 323 lineages.

324 **Figure 3 (A-B)** Minimum spanning networks of the hemagglutinin (HA) segment of H3N2 viral DNA
 325 from the *aedenet* package representing flu epidemics from 2001 to 2006 without reticulation (A) and with
 326 reticulation (B) (Jombart, 2008; Jombart et al., 2010). Each node represents a unique multilocus genotype,
 327 colors represent epidemic year, and edge color represents absolute genetic distance. (C) Shannon entropy
 328 values for population assignments compared with communities determined by the infoMAP algorithm on
 329 (A) and (B). (D) Graphic reproduced from Jombart et al. (2010) showing that the 2006 epidemic does not
 330 cluster neatly with the other years.

331 **Figure 4** UPGMA dendrogram generated from Nei's genetic distance on 15 breeds of *Bos taurus* (BT)
 332 or *Bos indicus* (BI) from Africa (AF) or France (FR). These data are from Laloë et al. (2007). Node labels
 333 represent bootstrap support $> 50\%$ out of 1,000 bootstrap replicates.

334 **Figure 5** Genotype accumulation curve for 694 isolates of the peach brown rot pathogen, *Monilinia*
 335 *fructicola* genotyped over 13 loci from Everhart and Scherm (2015). The horizontal axis represents the
 336 number of loci randomly sampled without replacement up to $n - 1$ loci, the vertical axis shows the number
 337 of multilocus genotypes observed, up to 262, the number of unique multilocus genotypes in the data set.
 338 The red dashed line represents 90% of the total observed multilocus genotypes. A trendline (blue) has
 339 been added using the *ggplot2* function *stat_smooth*.

340 **Figure 6 (A)** Sliding window analysis of the standardized index of association (\bar{r}_d) across a simulated
 341 1.1×10^4 nt chromosome containing 1,100 variants among 100 individuals. Each window analyzed
 342 variants within 500nt chunks. The black line refers to the clonal and the blue line to the sexual populations.
 343 **(B)** boxplots showing 100 random samples of 50 variants to calculate a distribution of \bar{r}_d for the clonal
 344 (red) and sexual (blue) populations. Each box is centered around the mean, with whiskers extending out
 345 to 1.5 times the interquartile range. The median is indicated by the center line. (A) and (B) are plotted on
 346 the same y-axis.

REFERENCES

- 347 Agapow, P.-M., and Burt, A. (2001). Indices of multilocus linkage disequilibrium. *Molecular Ecology Notes* 1, 101–102. doi:10.1046/j.1471-8278.2000.00014.x.
- 348 Anderson, J. B., and Kohn, L. M. (1995). Clonality in soilborne, plant-pathogenic fungi. *Annual review of phytopathology* 33, 369–391.
- 351 Arnaud-Hanod, S., Duarte, C. M., Alberto, F., and Serrão, E. A. (2007). Standardizing methods to
 352 address clonality in population studies. *Molecular Ecology* 16, 5115–5139.
- 353 Brown, A., Feldman, M., and Nevo, E. (1980). Multilocus structure of natural populations of *Hordeum*
 354 *spontaneum*. *Genetics* 96, 523–536. Available at: <http://www.genetics.org/content/96/2/523.abstract>.
- 356 Bruvo, R., Michiels, N. K., D'Souza, T. G., and Schulenburg, H. (2004). A simple method for the
 357 calculation of microsatellite genotype distances irrespective of ploidy level. *Molecular Ecology* 13, 2101–
 358 2106.

- 359 Chakarov, N., Linke, B., Boerner, M., Goesmann, A., Krüger, O., and Hoffman, J. I. (2015). Apparent
360 vector-mediated parent-to-offspring transmission in an avian malaria-like parasite. *Molecular ecology* 24,
361 1355–1363.
- 362 Cooke, D. E., Cano, L. M., Raffaele, S., Bain, R. A., Cooke, L. R., Etherington, G. J., Deahl, K. L.,
363 Farrer, R. A., Gilroy, E. M., Goss, E. M., et al. (2012). Genome analyses of an aggressive and invasive
364 lineage of the Irish potato famine pathogen. *PLoS pathogens* 8, e1002940.
- 365 Csardi, G., and Nepusz, T. (2006). The igraph software package for complex network research.
366 *InterJournal Complex Systems*, 1695. Available at: <http://igraph.org>.
- 367 Dagum, L., and Menon, R. (1998). OpenMP: An industry standard API for shared-memory
368 programming. *Computational Science & Engineering, IEEE* 5, 46–55.
- 369 Davey, J. W., and Blaxter, M. L. (2010). RADSeq: Next-generation population genetics. *Briefings in*
370 *Functional Genomics* 9, 416–423. doi:10.1093/bfgp/elq031.
- 371 Davey, J. W., Hohenlohe, P. A., Etter, P. D., Boone, J. Q., Catchen, J. M., and Blaxter, M. L.
372 (2011). Genome-wide genetic marker discovery and genotyping using next-generation sequencing. *Nature*
373 *Reviews Genetics* 12, 499–510.
- 374 Dobzhansky, T. (1973). Nothing in biology makes sense except in the light of evolution. *The American*
375 *Biology Teacher* 75, 87–91.
- 376 Elshire, R. J., Glaubitz, J. C., Sun, Q., Poland, J. A., Kawamoto, K., Buckler, E. S., and Mitchell, S. E.
377 (2011). A robust, simple genotyping-by-sequencing (GBS) approach for high diversity species. *Plos one*
378 6, e19379.
- 379 Everhart, S., and Scherm, H. (2015). Fine-scale genetic structure of *Monilinia fructicola* during brown
380 rot epidemics within individual peach tree canopies. *Phytopathology* 105, 542–549.
- 381 Excoffier, L., Smouse, P. E., and Quattro, J. M. (1992). Analysis of molecular variance inferred from
382 metric distances among DNA haplotypes: Application to human mitochondrial DNA restriction data.
383 *Genetics* 131, 479–491.
- 384 Falush, D., Stephens, M., and Pritchard, J. K. (2003). Inference of population structure using multilocus
385 genotype data: Linked loci and correlated allele frequencies. *Genetics* 164, 1567–1587. Available at:
386 <http://www.genetics.org/content/164/4/1567.abstract>.
- 387 Goss, E. M., Larsen, M., Chastagner, G. A., Givens, D. R., and Grünwald, N. J. (2009). Population
388 genetic analysis infers migration pathways of *Phytophthora ramorum* in US nurseries. *PLoS pathogens* 5,
389 e1000583.
- 390 Goss, E. M., Tabima, J. F., Cooke, D. E., Restrepo, S., Fry, W. E., Forbes, G. A., Fieland, V. J., Cardenas,
391 M., and Grünwald, N. J. (2014). The Irish potato famine pathogen *Phytophthora infestans* originated in
392 central Mexico rather than the Andes. *Proceedings of the National Academy of Sciences* 111, 8791–8796.
- 393 Goudet, J. (2005). Hierfstat, a package for R to compute and test hierarchical F-statistics. *Molecular*
394 *Ecology Notes* 5, 184–186.
- 395 Gross, A., Hosoya, T., and Queloz, V. (2014). Population structure of the invasive forest pathogen
396 *Hymenoscyphus pseudoalbidus*. *Molecular ecology* 23, 2943–2960.
- 397 Grünwald, N. J., and Goss, E. M. (2011). Evolution and population genetics of exotic and re-emerging
398 pathogens: Novel tools and approaches. *Annual Review of Phytopathology* 49, 249–267.
- 399 Grünwald, N. J., and Hoheisel, G.-A. (2006). Hierarchical analysis of diversity, selfing, and genetic
400 differentiation in populations of the oomycete *Aphanomyces euteiches*. *Phytopathology* 96, 1134–1141.

- 401 Grünwald, N. J., Goodwin, S. B., Milgroom, M. G., and Fry, W. E. (2003). Analysis of genotypic
402 diversity data for populations of microorganisms. *Phytopathology* 93, 738–46. Available at: <http://apsjournals.apsnet.org/doi/abs/10.1094/PHYTO.2003.93.6.738>.
- 403
- 404 Grünwald, N. J., Martin, F. N., Larsen, M. M., Sullivan, C. M., Press, C. M., Coffey, M. D., Hansen,
405 E. M., and Parke, J. L. (2011). Phytophthora-iD. org: A sequence-based phytophthora identification tool.
406 *Plant Disease* 95, 337–342.
- 407 Jombart, T. (2008). Adegenet: a R package for the multivariate analysis of genetic markers.
408 *Bioinformatics* 24, 1403–1405. doi:10.1093/bioinformatics/btn129.
- 409 Jombart, T., and Ahmed, I. (2011). Adegenet 1.3-1: New tools for the analysis of genome-wide SNP
410 data. *Bioinformatics* 27, 3070–3071.
- 411 Jombart, T., Devillard, S., and Balloux, F. (2010). Discriminant analysis of principal components: A
412 new method for the analysis of genetically structured populations. *BMC genetics* 11, 94.
- 413 Kamvar, Z. N., Larsen, M. M., Kanaskie, A. M., Hansen, E. M., and Grünwald, N. J. (2015). Spatial and
414 temporal analysis of populations of the sudden oak death pathogen in Oregon forests. *Phytopathology*, in
415 press.
- 416 Kamvar, Z. N., Larsen, M. M., Kanaskie, A. M., Hansen, E. M., and Grünwald, N. J. (2014a).
417 Sudden_Oak_Death_in_Oregon_Forests: Spatial and temporal population dynamics of the sudden oak
418 death epidemic in Oregon Forests. doi:10.5281/zenodo.13007.
- 419 Kamvar, Z. N., Tabima, J. F., and Grünwald, N. J. (2014b). Poppr: An R package for genetic analysis of
420 populations with clonal, partially clonal, and/or sexual reproduction. *PeerJ* 2, e281.
- 421 Laloë, D., Jombart, T., Dufour, A.-B., and Moazami-Goudarzi, K. (2007). Consensus genetic structuring
422 and typological value of markers using multiple co-inertia analysis. *Genetics Selection Evolution* 39, 1–23.
- 423 Lees, A., Wattier, R., Shaw, D., Sullivan, L., Williams, N., and Cooke, D. (2006). Novel microsatellite
424 markers for the analysis of *Phytophthora infestans* populations. *Plant Pathology* 55, 311–319.
- 425 Li, Y., Cooke, D. E., Jacobsen, E., and Lee, T. van der (2013). Efficient multiplex simple sequence repeat
426 genotyping of the oomycete plant pathogen *Phytophthora infestans*. *Journal of microbiological methods*
427 92, 316–322.
- 428 Linde, C., Zhan, J., and McDonald, B. (2002). Population structure of *Mycosphaerella graminicola*:
429 From lesions to continents. *Phytopathology* 92, 946–955.
- 430 Luikart, G., England, P. R., Tallmon, D., Jordan, S., and Taberlet, P. (2003). The power and promise of
431 population genomics: From genotyping to genome typing. *Nature Reviews Genetics* 4, 981–994.
- 432 Mantel, N. (1967). The detection of disease clustering and a generalized regression approach. *Cancer*
433 research 27, 209–220.
- 434 Mastretta-Yanes, A., Arrigo, N., Alvarez, N., Jorgensen, T. H., Piñero, D., and Emerson, B.
435 (2015). Restriction site-associated DNA sequencing, genotyping error estimation and de novo assembly
436 optimization for population genetic inference. *Molecular ecology resources* 15, 28–41.
- 437 McDonald, B. A., and Linde, C. (2002). The population genetics of plant pathogens and breeding
438 strategies for durable resistance. *Euphytica* 124, 163–180. doi:10.1023/A:1015678432355.
- 439 Meirmans, P. G., and Van Tienderen, P. H. (2004). GENOTYPE and GENODIVE: Two programs for
440 the analysis of genetic diversity of asexual organisms. *Molecular Ecology Notes* 4, 792–794.
- 441 Metzger, M. J., Reinisch, C., Sherry, J., and Goff, S. P. (2015). Horizontal transmission of clonal cancer
442 cells causes leukemia in soft-shell clams. *Cell* 161, 255–263.
- 443 Michalakis, Y., and Excoffier, L. (1996). A generic estimation of population subdivision using distances
444 between alleles with special reference for microsatellite loci. *Genetics* 142, 1061–1064.

- 445 Milgroom, M. G. (1996). Recombination and the multilocus structure of fungal populations. *Annual
446 review of phytopathology* 34, 457–477.
- 447 Milgroom, M. G., Levin, S. A., and Fry, W. E. (1989). Population genetics theory and fungicide
448 resistance. *Plant disease epidemiology* 2, 340–367.
- 449 Nei, M. (1973). Analysis of gene diversity in subdivided populations. *Proceedings of the National
450 Academy of Sciences* 70, 3321–3323.
- 451 Oksanen, J., Blanchet, F. G., Kindt, R., Legendre, P., Minchin, P. R., O'Hara, R. B., Simpson, G. L.,
452 Solymos, P., Stevens, M. H. H., and Wagner, H. (2015). *Vegan: Community ecology package*. Available
453 at: <http://CRAN.R-project.org/package=vegan>.
- 454 Paradis, E. (2010). Pegas: an R package for population genetics with an integrated-modular approach.
455 *Bioinformatics* 26, 419–420.
- 456 Prevosti, A., Ocaña, J., and Alonso, G. (1975). Distances between populations of *Drosophila
457 subobscura*, based on chromosome arrangement frequencies. *Theoretical and Applied Genetics* 45,
458 231–241.
- 459 R Core Team (2015). *R: A language and environment for statistical computing*. Vienna, Austria: R
460 Foundation for Statistical Computing Available at: <http://www.R-project.org/>.
- 461 Rosvall, M., and Bergstrom, C. T. (2008). Maps of random walks on complex networks reveal
462 community structure. *Proceedings of the National Academy of Sciences* 105, 1118–1123.
- 463 Shannon, C. (2001). A mathematical theory of communication. *ACM SIGMOBILE Mobile Computing
464 and Communications Review* 5, 3–55. Available at: <http://cm.bell-labs.com/cm/ms/what/shannonday/shannon1948.pdf>.
- 466 Smith, J. M., Smith, N. H., O'Rourke, M., and Spratt, B. G. (1993). How clonal are bacteria?
467 *Proceedings of the National Academy of Sciences* 90, 4384–4388. doi:10.1073/pnas.90.10.4384.
- 468 Sokal, R. R. (1958). A statistical method for evaluating systematic relationships. *Univ Kans Sci Bull* 38,
469 1409–1438.
- 470 Taylor, J. W., and Fisher, M. C. (2003). Fungal multilocus sequence typing — it's not just for bacteria.
471 *Current opinion in microbiology* 6, 351–356.
- 472 Wickham, H., and Chang, W. (2015). *Devtools: Tools to make developing R packages easier*. Available
473 at: <http://CRAN.R-project.org/package=devtools>.
- 474 Yoshida, K., Schuenemann, V. J., Cano, L. M., Pais, M., Mishra, B., Sharma, R., Lanz, C., Martin,
475 F. N., Kamoun, S., Krause, J., et al. (2013). The rise and fall of the *phytophthora infestans* lineage that
476 triggered the irish potato famine. *Elife* 2, e00731.